



University of  
Massachusetts  
Amherst

## Limits on Hot Galactic Halo Gas from X-Ray Absorption Lines

|               |   |
|---------------|---|
| Item Type     | article;article   |
| Authors       | Yao, Y;Nowak, MA;Wang, QD;Schulz, NS;Canizares, CR  |
| DOI           | <a href="https://doi.org/10.1086/526767">https://doi.org/10.1086/526767</a>                     |
| Download date | 2024-08-06 01:20:36   |
| Link to Item  | <a href="https://hdl.handle.net/20.500.14394/2632">https://hdl.handle.net/20.500.14394/2632</a> |

## LIMITS ON HOT GALACTIC HALO GAS FROM X-RAY ABSORPTION LINES

Y. YAO<sup>1</sup>, M. A. NOWAK<sup>1</sup>, Q. D. WANG<sup>2</sup>, N. S. SCHULZ<sup>1</sup>, AND C. R. CANIZARES<sup>1</sup>

Accepted for publication in the *ApJ Letters*

### ABSTRACT

Although the existence of large-scale hot gaseous halos around massive disk galaxies have been theorized for a long time, there is yet very little observational evidence. We report the *Chandra* and *XMM-Newton* grating spectral detection of O VII and Ne IX  $K\alpha$  absorption lines along the sight-line of 4U 1957+11. The line absorption is consistent with the interstellar medium in origin. Attributing these line absorptions to the hot gas associated with the Galactic disk, we search for the gaseous halo around the Milky Way by comparing this sight-line with more distant ones (toward LMC X-3 and the AGN Mrk 421). We find that all the line absorptions along the LMC X-3 and Mrk 421 sight-lines are attributable to the hot gas in a thick Galactic disk, as traced by the absorption lines in the spectra of 4U 1957+11 after a Galactic latitude dependent correction. We constrain the O VII column density through the halo to be  $N_{\text{OVII}} < 5 \times 10^{15} \text{ cm}^{-2}$  (95% confidence limit), and conclude that the hot gas contribution to the metal line absorptions, if existing, is negligible.

*Subject headings:* Galaxy: halo — Galaxy: structure — X-rays: individual (4U 1957+11, Mrk 421, LMC X-3)

### 1. INTRODUCTION

Many semi-analytic calculations and numerical simulations for disk galaxy formation predict the existence of extended hot gaseous halos around massive spirals due to the accretion of the intergalactic medium. For the Milky Way, the gas temperature can be shock-heated to  $\sim 10^6$  K at the virial radius ( $\sim 250$  kpc; e.g., Birnboim & Dekel 2003; Fukugita & Peebles 2006), and the total mass contained in the large scale halo can be comparable with or even greater than the total baryonic mass of stars and the interstellar medium in the Galactic disk (e.g., Sommer-Larsen 2006). Clearly, an observational measurement of such an extended halo will provide an important test of galaxy formation theories.

Searching for X-ray emission from large scale halos around nearby disk galaxies has proven unsuccessful. Extraplanar X-ray emissions have indeed been routinely detected around a number of nearby spirals, but only on scales of several kpc (except for the star burst galaxies), and most likely as the result from on-going stellar feedback in galactic disks (e.g., Tüllmann et al. 2006; Li et al. 2006). The X-ray surface brightness of a galactic halo must be very weak at large scales, at least partly because of the density square dependence of the emission and the possible low metallicity of the gas. So far, the only claimed detection of an apparent X-ray-emitting halo on a scale of  $\sim 20$  kpc is around the quiescent edge-on disk galaxy NGC 5746 (Pedersen et al. 2006).

The large-scale hot gaseous halo around the Milky Way is indirectly evidenced by the presence of high velocity clouds (HVCs), in particular, the detection of their associated O VI line absorption (e.g., Spitzer 1956; Sembach et al. 2003). Because the O VI-bearing gas is preferentially populated at intermediate temperatures of  $\sim 3 \times 10^5$  K where thermally unstable cooling occurs, it is believed to be produced at the interfaces between the cold/warm and the hot media. Without knowing the temperature distribution and the metallicity of the hot gas, however, it is very hard to reliably estimate its

total mass.

The best way to directly measure the hot medium is through its X-ray absorption line features. Indeed, O VII, O VIII, and/or Ne IX absorption lines consistent with zero velocity shifts ( $cz \sim 0$ ) have been detected unambiguously toward several bright extragalactic sources (e.g., LMC X-3, Mrk 421, and PKS 2155-304; Nicastro et al. 2002; Fang et al. 2003; Wang et al. 2005; Yao & Wang 2007a, YW07a hereafter). But these sight-lines pass through the Galactic disk, the extended Galactic halo, and (for those AGNs) the possible warm hot intergalactic medium (WHIM) in the Local Group. Recently, it has been argued that the bulk of these absorptions can *not* be produced in the WHIM (Fang et al. 2006; Yao & Wang 2007a; Bregman & Lloyd-Davies 2007). Indeed, these highly ionized absorption lines have also been detected in spectra of many Galactic sources (e.g., Yao & Wang 2005; Juett et al. 2006), clearly indicating the existence of the hot gas in the Galactic disk. All existing X-ray absorption and emission data are consistent with the hot gas located in the Galactic disk with a vertical exponential scale height of  $\sim 2$  kpc (Yao & Wang 2005, 2007a), comparable to those inferred from the angular distributions of column densities of the O VI-bearing gas and pulsar dispersion measures (Savage et al. 2003; Berkhuijsen et al. 2006). Clearly, the constraint on the location of the hot gas depends on the modeling. For instance, Bregman & Lloyd-Davies (2007) found that the absorbing gas toward AGNs are also consistent with a uniformly spherical distribution within a radius of 20 kpc. The questions here are, whether the extended Galactic halo (defined as the hot gas in the region of  $> 10$  kpc beyond the Galactic plane but within the Galactic virial radius) exists, and how much does it contribute to the observed highly ionized X-ray absorptions?

In this Letter, we present a differential study searching for such a large-scale hot gaseous halo around our Galaxy by comparing observations between sight-lines of 4U 1957+11 and Mrk 421, and between those of LMC X-3 and Mrk 421. Ne IX, O VII, and/or O VIII absorption lines at  $cz \sim 0$  have been detected in spectra of all three sources observed with *Chandra* and/or *XMM-Newton X-ray Observatories*. These comparisons enable us to probe the Galactic halo by examining its contribution to the observed absorption lines, and then to estimate its total mass and/or its metallicity.

<sup>1</sup> Massachusetts Institute of Technology (MIT) Kavli Institute for Astrophysics and Space Research, 70 Vassar Street, Cambridge, MA 02139; yaoy, mnnowak, nss, and crc@space.mit.edu

<sup>2</sup> Department of Astronomy, University of Massachusetts, Amherst, MA 01003; wqd@astro.umass.edu

Throughout the Letter, we adopt the solar abundances from Wilms et al. (2000), quote statistical errors (or upper limits) for single floating parameters at 90% (95%) confidence levels, and assume that the hot gas in both the Galactic disk and halo is in the collisional ionization equilibrium state and is approximately isothermal. We further assume that the disk gas is distributed following an exponential decay law with a vertical scale height of 2 kpc (e.g., Savage, et al. 2003; YW07a). All the data analyses are performed with the software package XSPEC (version 11.3.2).

## 2. OBSERVATIONS AND DATA REDUCTION

4U 1957+11 (V1408 Aquilae;  $l, b = 51^\circ 31', -9^\circ 33'$ ) is a persistent low mass X-ray binary (Nowak & Wilms 1999 and references therein). *Chandra* observed this source for 67 ks on 2004 September 7 (ObsID 4552) with the High Energy Transmission Grating Spectrometer (HETGS; Canizares et al. 2005) and *XMM-Newton* observed it for 45 ks on 2004 October 16 (ObsID 206320101).

We reprocessed both *Chandra* and *XMM-Newton* observations following the standard procedures. Using the software package CIAO<sup>3</sup> and calibration database (CALDB) version 3.4, we re-calibrated the *Chandra* observation, extracted grating spectra, and calculated corresponding instrumental response files (RSPs). In this study, we only use the first order spectra from the medium energy grating because of its large effective area at longer wavelengths ( $> 13 \text{ \AA}$ ). To further enhance the counting statistics, we co-added the positive- and the negative-grating spectra and RSPs. For the *XMM-Newton* observation, we used the software package SAS (version 6.50)<sup>4</sup> to remove those events contaminated with background flares (by screening out the time intervals with an event count rate  $> 0.4$  counts/s on the CCD9), and then extracted spectra and calculated RSPs from the Reflection Grating Spectrometer (RGS) events by running the thread *rgsproc*. Because of the failure of the CCD4 in the RGS2, we only use the RGS1 spectrum.

In order to measure absorption line properties we only rely on the nearby continuum levels. We therefore use several parts of the spectra that are local to the lines of our interest. For the *Chandra* spectrum, we use a wavelength range of 12.0–22.5  $\text{\AA}$  covering the  $K\alpha$  and/or  $K\beta$  transition lines of O VII, O VIII, Ne VIII, Ne IX, and Ne X. For the case of the *XMM-Newton* spectrum, the RGS1 has no effective area around the Ne IX  $K\alpha$  line and there is a bad pixel near the O VIII  $K\alpha$  line at 18.969  $\text{\AA}$ . Here we use ranges of 18.0–18.9 and 19.2–22.5  $\text{\AA}$  covering the O VII  $K\alpha$  and  $K\beta$  lines.

Mrk 421, a bright quasar at  $z = 0.03$  ( $l, b = 179^\circ 83', 65^\circ 03'$ ), is a *Chandra* calibration target and has been observed with the high resolution grating instruments multiple times; most of the observations have been reported in YW07. In this Letter, we use the same observations, and the same spectra and RSPs as in YW07. To fit the spectra without worrying about overlapping spectral orders, for each of the observations taken with High Resolution Camera (HRC; Table 1 in YW07), we derive the first order spectrum with minimal higher ( $> 1$ ) order confusion via the following steps. We first fit the broadband (1.5–35  $\text{\AA}$ ) order-overlapped spectrum with the order combined RSP, and then multiply the spectral counts channel by channel with the ratio between the model predicated

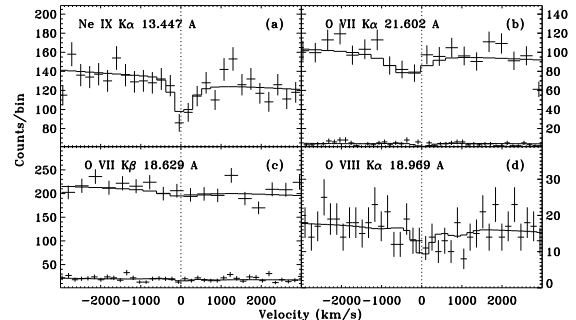


FIG. 1.— The oxygen and neon absorption lines detected in the spectra of 4U 1957+11. The upper plots in panels (b) and (c) are from the *XMM-Newton* spectrum; the others are from the *Chandra* spectrum. The vertical dotted lines mark zero velocity. The bin-size is 22.2 m $\text{\AA}$  and 10.0 m $\text{\AA}$  for *XMM-Newton* and *Chandra* spectra, respectively.

counts based on the first order RSP and that based on the order-combined RSP. We then combine all the first order spectra of different observations using the same procedure as in YW07.

In YW07, we have reported the O VII  $K\alpha$ ,  $K\beta$ , and O VIII  $K\alpha$  absorption lines in the spectrum of Mrk 421 and measured their equivalent widths (EWs; see also Williams et al. 2005; Kaastra et al. 2006). In fact, the Ne IX  $K\alpha$  line has also been detected in the spectrum (Williams et al. 2005). However, we find that, due to an instrumental feature near the line, measuring the amount of the Ne IX absorption is severely affected by how the continuum is placed. To avoid such an uncertainty, in our analysis we only use the spectral range of 18–22.5  $\text{\AA}$ , covering the oxygen lines as mentioned above.

LMC X–3 ( $l, b = 273^\circ 58', -32^\circ 08'$ ) is located  $\sim 50$  kpc away from the Sun and *Chandra* observed it with the Low Energy Transmission Grating Spectrometer plus HRC for  $\sim 100$  ks in total. The interstellar O VII and Ne IX  $K\alpha$  absorption lines observed in this sight-line have been reported by Wang et al. (2005). In this Letter, we use the same spectra and RSPs as in Wang et al. . Following the same procedure as for Mrk 421 spectra (see above), we obtained the co-added first order spectrum and the RSP. We use the spectral range of 12.0–22.5  $\text{\AA}$  in the following analysis.

## 3. ANALYSIS AND RESULTS

We focus our efforts on searching for and analyzing the highly ionized absorption lines at  $cz \sim 0$  that are likely produced in the hot ISM (§ 4). The Ne IX (13.447  $\text{\AA}$ ) and O VII  $K\alpha$  (21.602  $\text{\AA}$ ) lines consistent with  $cz \sim 0$  appear in the *Chandra* and *XMM-Newton* spectra at  $\sim 3$  and  $4\sigma$  significance levels (Fig. 1), respectively. Modeling these two lines with negative Gaussian models, we measure their EWs as 6.3(3.9, 8.8) and 18.7(8.3, 30.6) m $\text{\AA}$ . Note that the EWs measured here are for reference only. The ionic column density and the dispersion velocity of the absorbing gas will be measured in below. No other highly ionized O and Ne lines are detected at  $\gtrsim 2\sigma$  significance. Fixing the line centroid at the rest frame wavelength (Verner et al. 1996; Behar & Netzer 2002), we obtain the EW upper limits of Ne X(12.134  $\text{\AA}$ ), Ne VIII (13.646  $\text{\AA}$ ) and O VIII  $K\alpha$  (18.969  $\text{\AA}$ ), and O VII  $K\beta$  (18.629  $\text{\AA}$ ) lines as 1.2, 2.8, 15.6, 10.1 m $\text{\AA}$ , respectively. Since all these line are unresolved, we fix the line width  $\sigma$  to 100 km s $^{-1}$  (please refer to  $v_b$  in Table 1) during these measurements and we use either the *Chandra* or *XMM-Newton* spectrum, whichever has higher counting statistics near the line (Fig. 1).

A comparison of the line absorption between 4U 1957+11

<sup>3</sup> <http://cxc.harvard.edu/ciao/>

<sup>4</sup> <http://xmm.vilspa.esa.es/sas/current/documentation/threads>

TABLE 1  
LINE ANALYSIS RESULTS

|                      | $T$<br>( $10^6$ K) | $v_b$<br>( $\text{km s}^{-1}$ ) | $N_{\text{OVII}}$<br>( $10^{15} \text{ cm}^{-2}$ ) | $N_{\text{HAO}}$<br>( $10^{19} \text{ cm}^{-2}$ ) |
|----------------------|--------------------|---------------------------------|--|---|
| Mrk 421 <sup>a</sup> | 1.4(1.3, 1.6)      | 64(48, 104)                     | 10.0(6.6, 14.7)                                    | 1.4(1.0, 2.0)                                     |
| 4U 1957 <sup>a</sup> | 2.2(1.6, 2.7)      | 155(70, 301)                    | 3.1(1.8, 8.2)                                      | 1.1(0.6, 1.8)                                     |
| LMC X3 <sup>a</sup>  | 1.3(0.8, 2.0)      | 79(62, 132)                     | 11.7(7.4, 18.5)                                    | 2.3(1.5, 3.7)                                     |
| 4U 1957 <sup>b</sup> | 1.8(1.7, 2.1)      | 70(50, 172)                     | 7.0(3.2, 12.7)                                     | 1.4(0.7, 2.2)                                     |
| Halo <sup>c</sup>    | ...                | ...                             | < 4.8  | < 0.9   |
| LMC X3 <sup>b</sup>  | 1.8(1.6, 2.0)      | 64(49, 108)                     | 8.8(5.8, 12.7)                                     | 1.7(1.2, 2.2)                                     |
| Halo <sup>c</sup>    | ...                | ...                             | < 3.7  | < 0.7   |

NOTE. — The uncertainty ranges (upper limits) are quoted at 90% (95%) confidence levels. The dependence of the column density on the Galactic latitude ( $\sin b$  factor) has been corrected with respect to Mrk 421 direction.  $A_{\text{O}}$  is the oxygen abundance in unit of the solar value. <sup>a</sup> Results from fitting lines in each direction separately. <sup>b</sup> Results from a joint analysis of lines in the source and those in Mrk 421. <sup>c</sup> The absorption contribution from the halo gas beyond the source. See text for detail.

and Mrk 421 sight-lines provides an effective probe of the large scale Galactic hot gaseous halo. The distance of 4U 1957+11 is estimated to be  $D \sim 10 - 25$  kpc (M. Nowak et al. in preparation), a location of 1.6 – 4.1 kpc below the Galactic disk plane where it samples 55-87% of the Galactic disk gas in the vertical direction (§ 1) along the line of sight. In comparison, the line of sight towards Mrk 421 samples the hot gas not only in the Galactic disk but also in the putative Galactic halo (§ 1). Therefore the differential absorptions between these two sight-lines allow us to directly constrain the absorption contribution from the halo.

We first characterize the hot absorbing gas towards these two sight-lines by using our absorption line model, *absline*. This model adopts the the *Voigt* function to approximate an individual line profile, and uses the line centroid  $E_l$ , velocity dispersion  $v_b$ , absorbing gas temperature  $T$ , and reference ionic column density  $N_X$  (e.g.,  $X = \text{O VII}$  or  $\text{H}$ ) as fitting parameters. It therefore can be used to conduct a joint analysis of multiple absorption lines (including non-detections).<sup>5</sup> For the sight-line toward Mrk 421, we use O VII  $K\alpha$ ,  $K\beta$ , and O VIII  $K\alpha$  absorption lines from the *Chandra* spectrum (YW07). For sight-line toward 4U 1957+11, we use O VII, O VIII, Ne VIII, Ne IX, Ne X  $K\alpha$ , and O VII  $K\beta$  lines in the *Chandra* and *XMM-Newton* spectra where applicable, and assume the neon to oxygen abundance ratio to be the solar value (Yao & Wang 2006). From the joint analysis, we obtain the  $T$ ,  $v_b$ , and  $N_{\text{OVII}}$  (or its equivalent  $N_{\text{H}}$  for a given metallicity), as reported in Table 1. For ease of comparison, we take into account the dependence of the column density on the Galactic latitude ( $\sin b$  factor; § 1) for the 4U 1957+11 sight-line with respect to the Mrk 421 direction (Table 1).

Please note that in the above characterization we assume that the intervening hot gas in both sight-lines is isothermal. In reality, the temperature of both the disk and the halo gas could be a function of the vertical off-plane distance, the radial off-Galactic center distance, or a combination of both (e.g., Toft et al. 2002; YW07). This simplified description aims to provide a direct comparison of the amount of absorption between the two sight-lines.

As demonstrated in Table 1 and Figure 2, the absorption towards 4U 1957+11 can account for the bulk of the absorption towards Mrk 421. To quantify the absorption contribution from the putative Galactic halo gas, we jointly analyze the ab-

<sup>5</sup> Please refer to Yao & Wang (2005, 2006) for the model and the joint analysis procedure.

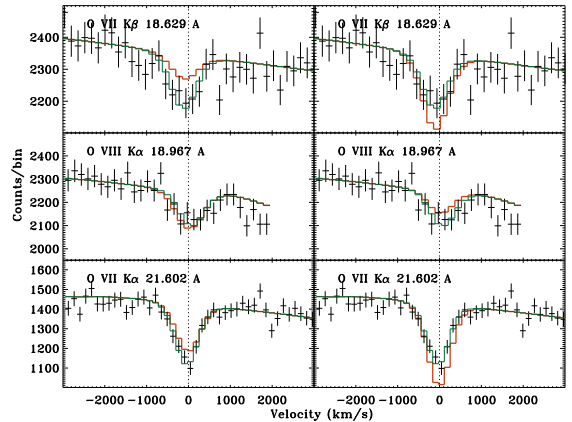


FIG. 2.— The observed Mrk 421 spectrum (cross) around the oxygen absorption lines and the best fit model (green histogram) convolved with the instrumental response. The red histograms mark the amount of absorption predicted for the Mrk 421 direction from the best fit of the lines observed in the spectra of 4U 1957+11 (left panels) and LMC X-3 (right panels).

sorption lines in these two directions, “subtract” the absorption spectrum toward 4U 1957+11 direction from that toward Mrk 421 direction, and attribute the residual absorption to the halo gas. We find that the halo gas is consistent with *no* contribution to the observed line absorptions. Assuming that the halo gas has the same thermal (e.g.,  $T$ ) and dynamic (e.g.,  $v_b$ ) properties as the disk gas, we estimate the column density upper limit of the halo gas as  $N_{\text{OVII}} < 4.8 \times 10^{15} \text{ cm}^{-2}$  (or  $N_{\text{HAO}} < 9 \times 10^{18} \text{ cm}^{-2}$ , where  $A_{\text{O}}$  is the oxygen abundance in unit of the solar value; Table 1). The halo gas and the disk gas may have different  $T$ ; for the halo gas over a broad temperature range of  $0.4 - 2.5 \times 10^6$  K, we find  $N_{\text{HAO}} < 10^{19} \text{ cm}^{-2}$ .

Following the same procedure as above, we characterize the line absorptions toward LMC X-3 (Table 1; see also Wang et al. 2005), and then search for the absorption feature of the halo gas beyond LMC X-3 by comparing it with Mrk 421. Again, we find that the line absorptions toward LMC X-3 can account for all the absorptions observed toward the Mrk 421 sight-line (Fig. 2), and obtain the upper limits of the column density of the halo by jointly analyzing the sight-lines of LMC X-3 and Mrk 421 (Table 1).

#### 4. DISCUSSION

In this study, we have assumed that the absorption lines observed in the spectra of 4U 1957+11 are produced in the ISM. However, the photo-ionized in- or out-flow material intrinsic to 4U 1957+11 could contaminate these lines. From the best fit to the *Chandra* spectrum in the range of 2–23 Å, we estimate the source luminosity over 0.5–10 keV as  $L = 1.19 D_{10\text{kpc}}^2 \times 10^{37} \text{ ergs s}^{-1}$ , where  $D_{10\text{kpc}}$  is the source distance in units of 10 kpc. A curve of growth analysis with a dispersion velocity ( $v_b$ ) of 0  $\text{km s}^{-1}$  gives a firm upper limit of the Ne IX column density to be  $N_{\text{NeIX}} < 6.6 \times 10^{17} \text{ cm}^{-2}$  (assuming the solar abundance of Ne). This is equivalent to a hydrogen column density  $N_{\text{H}} < 1.1 \times 10^{22} \text{ cm}^{-2}$ , assuming an ionization fraction of 0.5 for Ne IX. For the absorber, the ionization parameter  $U = L_x/n(r)r^2$  must satisfy  $\log(U) \leq 2.5$ , since the Ne X  $K\alpha$  absorption line has not been detected (Kallman & McCray 1982). Further assuming a radial gas density distribution  $n(r) \propto (r_w/r)^2$ , where  $r_w$  is the location where wind launches and  $r > r_w$ , we obtain  $r_w > 50R_{\odot}$ , which is much larger than the star separation ( $\lesssim 6R_{\odot}$ ) of the system (estimated from its orbital period 9.33 hours and taking an upper limit of the X-ray compact object  $M_X < 16M_{\odot}$ ).

These estimates make the in-flow scenario very unlikely. On the other hand, if the absorber is out-flow material, the lines are expected to be blue-shifted at velocities larger than the escape velocity of the system (e.g., GRO J1655–40; Miller et al. 2006), which is  $260 \text{ km s}^{-1}$  for 4U 1957+11 (taking  $M_X = 10M_\odot$  and  $r_w = 6R_\odot$ ). In contrast, the detected Ne IX  $K\alpha$  velocity is  $0 \pm 114 \text{ km s}^{-1}$ . The above arguments suggest that the absorption lines are more likely produced in the ISM (see also Juett et al. 2006), although the intrinsic scenario can not be completely ruled out.

We have compared the highly ionized line absorptions of O VII, O VIII, and Ne IX observed in the spectra of 4U 1957+11 and Mrk 421, and in the spectra of LMC X–3 and Mrk 421 to search for the large scale Galactic halo. We found that there is no significant X-ray absorption due to hot gas beyond either 4U 1957+11 or LMC X–3. These results are consistent with our previous conclusion that bulk of the absorptions observed toward the Mrk 421 sight-line are due to the hot gas around the Galactic disk with a scale height of  $\sim 2 \text{ kpc}$  based on a joint analysis of the absorption and emission data (YW07). Note that the upper limits obtained toward LMC X–3 are slightly lower than those toward 4U 1957+11 (Table 1). Some of the difference are due to the partial sampling of the Galactic disk by the latter sight-line, and the better spectral quality of LMC X–3 also matters.

Large scale hot gaseous halos are commonly expected in modern disk formation models for massive spirals (e.g. White & Frenk 1991). For the Milky Way in particular, the hot gaseous halo can extend up to  $r_{\text{virial}} \sim 250 \text{ kpc}$  and the total mass contained is expected to be  $\sim 6 \times 10^{10} M_\odot$ , which is currently missing in the baryon mass inventory in the Lambda Cold Dark Matter ( $\Lambda$ CDM) cosmology (Dehnen & Binney 1998; Klypin et al. 2002; Sommer-Larsen 2006). Recently, Maller & Bullock (2004) assumed that the fragmented warm clouds could be formed out of the hot gas halo and proposed a multiphase cooling scenario for the galaxy formation. This model alleviates the so-called “over-cooling” problem faced by the standard cooling model (e.g., Klypin et al. 2002). They then obtained a density profile for the residual hot halo gas as a function of radius (Eq. 21 and Fig. 4 in Maller & Bullock 2004). Normalizing their density profile by requiring the total column density integrated from 10 to 250 kpc to be  $N_{\text{H}A_0} < 10^{19} \text{ cm}^{-2}$  (Table 1), we obtain the total mass contained in the halo as  $M_{\text{H}} < 1.2/A_0 \times 10^{10} M_\odot$ . Clearly, to match this upper limit with the total missing baryon mass in the MW,  $A_0$  should be  $< 20\%$  of the solar

value. More recently, Hansen & Sommer-Larsen (2006) assumed that gaseous halos of galaxies are in a hydrostatic equilibrium state and that the gas density and the total mass density profiles are power laws, and then derived a hot halo gas density profile for the MW-like galaxy (Fig. 2 in Hansen & Sommer-Larsen 2006). Again, normalizing their profile we obtain the total hot gas mass as  $< 2.2/A_0 \times 10^9 M_\odot$ , requiring  $A_0$  to be  $< 3.7\%$  of the solar value.

Low metallicity of the hot halo gas is not surprising; the halo gas is believed to be primarily accreted from the intergalactic medium that is expected to be metal poor. This would also suggest that the star formation and the associated stellar feedback via Type II supernovae (SNeII) that occurred in the Galactic disk and bulge are not important in regulating the metal content of the halo. Hot gas resulting from SNeII, if leaking into the halo (e.g., Mac Low & Ferrara 1999), may cool quickly enough (via adiabatic expansion and atomic line radiation) to form metal-rich cold clouds in the local environment before homogenizing with the halo gas (Wang 2007). As these clouds return back to the disk plane as Galactic fountains, their interaction with the embedding hot gas could be another mechanism of warm cloud formation as required in multiphase cooling scenarios (Maller & Bullock 2004). The interfaces between these two media may harbor the bulk of HVCs as observed via O VI absorptions at large distance (e.g., Sembach et al. 2003).

In this Letter, we derive the mass and metallicity limits on the putative Galactic halo by comparing the observed absorption lines among the sight-lines of 4U 1957+11, LMC X–3, and Mrk 421. However, the amount of absorptions observed along different AGN sight-lines could vary substantially (e.g., Bregman & Lloyd-Davies 2007), which may be due to additional absorption components (e.g., 3C 273; Yao & Wang 2007b) and/or different absorbing gas properties. More comparisons among other sight-lines are therefore needed to confirm the presented results.

We are grateful to Li Ji and the anonymous referee for their insightful comments, which helped to improve the presentation of the paper. This work is supported by NASA through the Smithsonian Astrophysical Observatory contract SV3-73016 to MIT for support of the Chandra X-Ray Center under contract NAS 08-03060. Support from SAO/CXC grants AR6-7023 and AR7-8014 are also acknowledged.

#### REFERENCES

- Behar, E., & Netzer, H. 2002, *ApJ*, 570, 165  
 Berkhuijsen, E., et al. 2006, *AN*, 327, 82  
 Birnboim, Y., & Dekel, A. 2003, *MNRAS*, 345, 349  
 Bregman, J. N., & Lloyd-Davies, E. J. 2007, *ApJ* in press, astro-ph/07071699  
 Canizares, C. R., et al. 2005, *PASP*, 117, 1144  
 Dehnen, W., & Binney, J., 1998, *MNRAS*, 294, 429  
 Fang, T., et al. 2003, *ApJ*, 586, 49  
 Fang, T., et al. 2006, *ApJ*, 644, 174  
 Fukugita, M., & Peebles, P. 2006, *ApJ*, 639, 590  
 Hansen, S., & Sommer-Larsen, J. 2006, *ApJ*, 653, L17  
 Juett, A., et al. , 2006, *ApJ*, 648, 1066  
 Kaastra, J. S., Werner, N., den Herder, J. W. A., et al. 2006, 652, 189  
 Kallman, T. R., & McCray, R. 1982, *ApJS*, 50, 263  
 Klypin, A., Zhao, H., & Somerville, R. S. 2002, *ApJ*, 573, 597  
 Li, Z., et al. 2006, *MNRAS*, 371, 147  
 Maller, A. H., & Bullock, J. 2004, *MNRAS*, 355, 694  
 Mac Low, M., & Ferrara, A. 1999, *ApJ*, 513, 142  
 Miller, J., et al. 2006, *Nature*, 441, 953  
 Nicastro, F., et al. 2002, *ApJ*, 573, 157  
 Nowak, M. A., & Wilms, J. 1999, *ApJ*, 522, 476  
 Pedersen, K., et al. 2006, *New A.*, 11, 465  
 Savage, B., et al. 2003, *ApJS*, 146, 125  
 Sembach, K., et al. 2003, *ApJS*, 146, 165  
 Sommer-Larsen, J. 2006, 644, L1  
 Spitzer, L. 1956, *ApJ*, 124, 20  
 Toft, S., et al. 2002, *MNRAS*, 335, 799  
 Tüllmann, R, et al. 2006, *AA*, 448, 43  
 Verner, D. A., et al. 1996, *Atomic Data & Nuclear Data Tables*, 64, 1-180  
 Wang, Q. D., et al. 2005, *ApJ*, 635, 386  
 Wang, Q. D. 2007, *EAS*, 24, 59  
 Williams, R., Mathur, S., & Nicastro, F., et al. 2005, *ApJ*, 631, 856  
 Wilms, J., Allen, A., & McCray, R. 2000, *ApJ*, 542, 914  
 White, S. D. M., & Frenk, C. S. 1991, *ApJ*, 379, 52  
 Yao, Y., & Wang, Q. D., 2005, *ApJ*, 624, 751  
 Yao, Y., & Wang, Q. D., 2006, *ApJ*, 641, 930  
 Yao, Y., & Wang, Q. D., 2007a, *ApJ*, 658, 1088  
 Yao, Y., & Wang, Q. D., 2007b, *ApJ*, 666, 242